# MINERAL REACTIONS AND STRAIN LOCALIZATION IN A SHEARED MAFIC GRANULITE INFILTRATED BY MELT

G. degli Alessandrini* [1], L. Menegon [1], N. Malaspina [2], A. Dijkstra [1], M. Anderson [1]

* giulia.deglialessandrini@plymouth.ac.uk

[1] School of Geography, Earth and Environmental Sciences, Plymouth University, UK

[2] Department of Earth and Environmental Sciences, Universita' degli Studi di Milano Bicocca, Piazza della Scienza 4, 20126 Mi, Italy

## RESEARCH HIGHLIGHTS

This study investigates the deformation mechanisms in a continental lower-crust shear zone through detailed microstructural and EBSD analysis of a mafic dyke experiencing melt infiltration during shearing (Panel 1).

Opx porphyroclasts show evidence of crystal plasticity while cpx and plagioclase porphyroclasts show evidence of micro-cracking and micro-boudinage; both generally lack recovery features (subgrains) which is remarkable at ≈800°C (Panel 3-4-5-6).

The poly-phase matrix (grain size below 10μm) deforms by grainsize-sensitive creep (GSSC) (Panel 7).

How did the matrix form? Evidence of melt-rock interaction during shearing suggests matrix nucleation from melt-assisted metamorphic reactions (Panel 9.)

Melt assisted nucleation of fine grained matrix, deforming by GSSC, is responsible for major rheological weakening. Strain partitioning in the matrix imposes high strain rates, which results in local microcracking and microboudinage of the porphyroclasts.

## 2. SAMPLE MICROSTRUCTURAL OVERVIEW

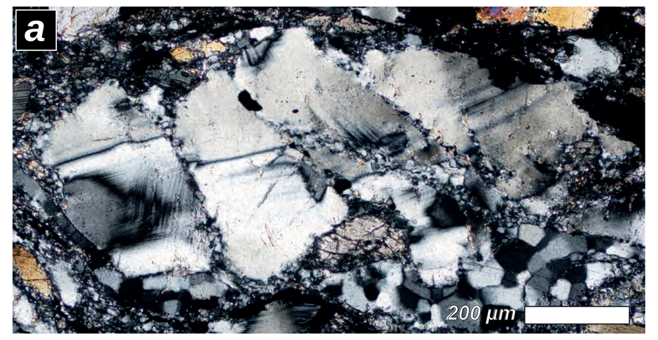

Fig. 2a - Optical micrograph of plagioclase porphyroclast displaying intracrystalline bands of recrystallized plagioclase, oriented antithetically to the sinistral sense of shear.

Fig. 2b - Optical micrograph of clinopyroxene crosscut by intracrystalline bands of fine-grained plagioclase.

Fig. 2c - SEM backscatter image of the mylonitic mafic dyke, with porphyroclasts of clinopyroxene, orthopyroxene and plagioclase in a fine polyphase matrix. Pyroxenes show evidence of micro-boudinage.

Fig. 2d - SEM backscatter image of elongated orthopyroxene porphyroclasts with aspect ratios up to 12.

Fig. 2e - Fine grained poly-phase matrix of opx + cpx + ilm + qtz + pl + kfs that wraps around the porphyroclasts, making ca 57% of the whole rock. Average grain size 5-7 μm.

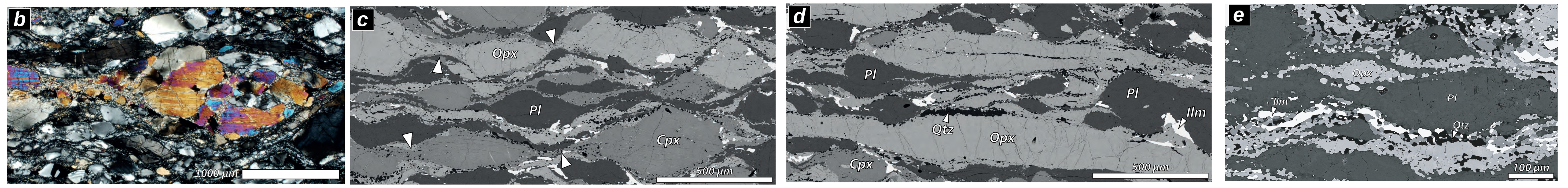


## 1. GEOLOGICAL SETTING

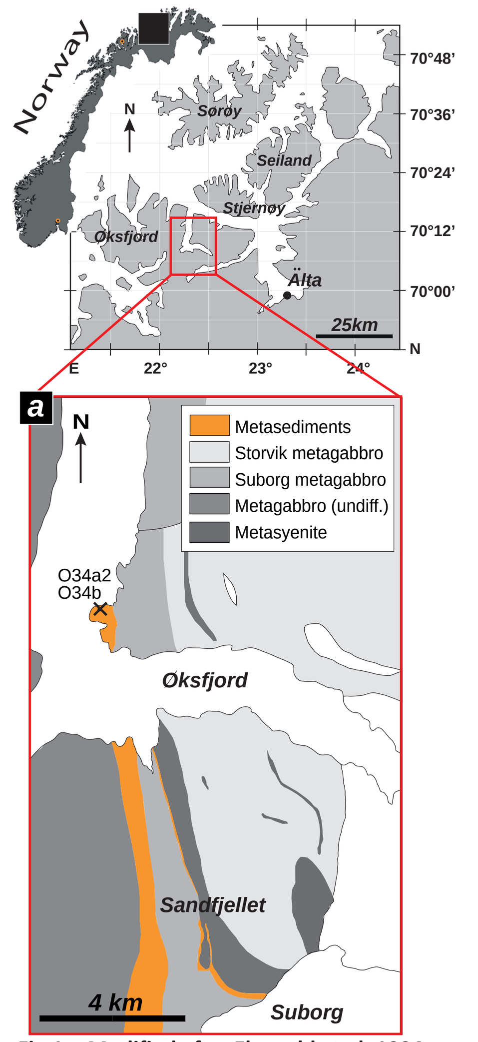


Fig.1a: Modified after Elvevold et al. 1994 and Reginiussen et al. 1995

**SEILAND IGNEOUS PROVINCE (N NORWAY)**

Magmatic province in N Norway with gabbros (Fig. 1a, grey) emplaced in lower crust metasediments (Fig. 1a, orange).

The studied sample is a former mafic dyke in the series of metapelites (Fig. 1b). Gabbro emplacement was accompanied by shearing and partial melting of host metasediments and mafic dykes.

Deformation conditions:
T =760 – 820°C and P = 0.75 – 0.95 GPa (Menegon et al. 2011)

At the P, T conditions of deformation, the mafic dykes did not undergo partial melting but there is evidence of melt infiltration from metapelites. Melt infiltration is evident at the outcrop scale(Fig. 1c) as well as at the thin-section scale (Fig. 1d-e)

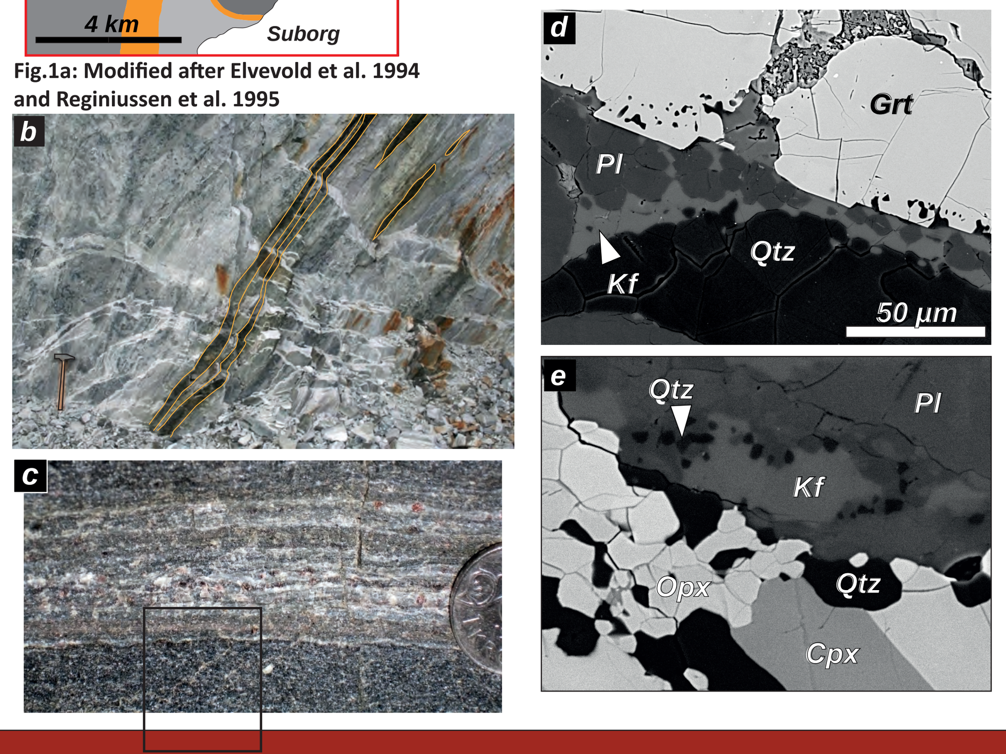


## 3. DEFORMATION MICROSTRUCTURES AND CRYSTALLOGRAPHIC PREFERRED ORIENTATIONS (CPO)

### 4. ORTHOPYROXENE PORPHYROCLASTS

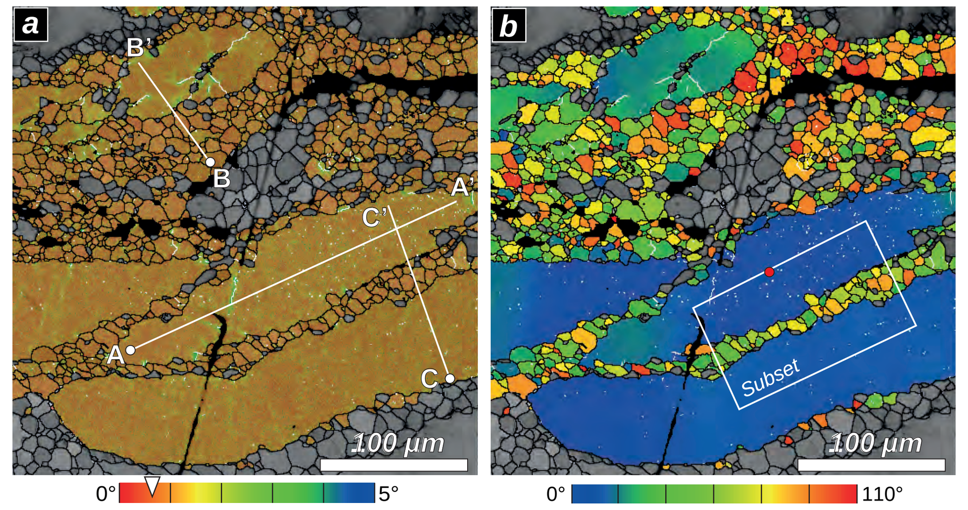


LOCAL MISORIENTATION MAP

**CRYSTALLOGRAPHIC ORIENTATION OF ORTHOPYROXENE**

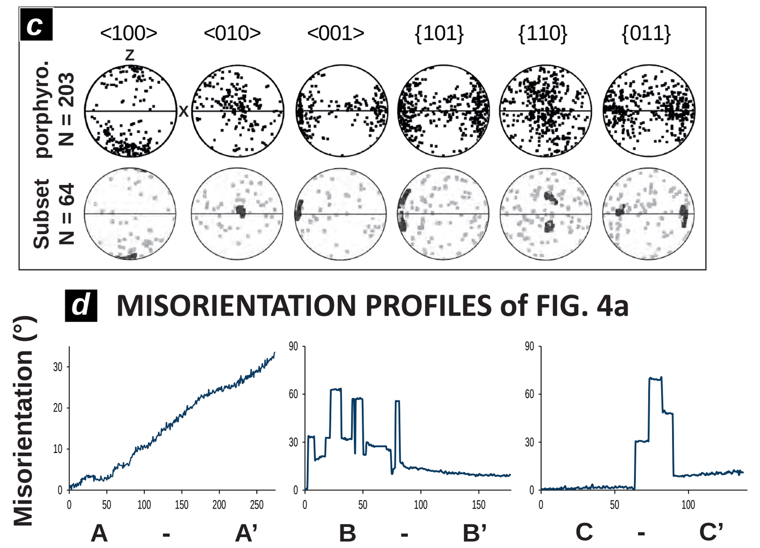


Orthopyroxene porphyroclasts preferentialy deform by dislocation glide on the {100}[001] slip system (Fig 4c).

There is no evidence for dynamic recrystallization as the porphyroclasts lack subgrains (Fig. 4a boundaries in white) and the fine grained aggregate rimming the porphyroclasts is highly misoriented and lacking a CPO (Fig. 4b - misorientations 40-60deg from red dot and Fig. 4c)

Porphyroclasts gradually accumulate lattice distortions up to 30deg (Profile A-A') whereas the fine grained aggregate corresponds to jumps in misorientation (Fig. 4d).

### 5. PLAGIOCLASE PORPHYROCLASTS

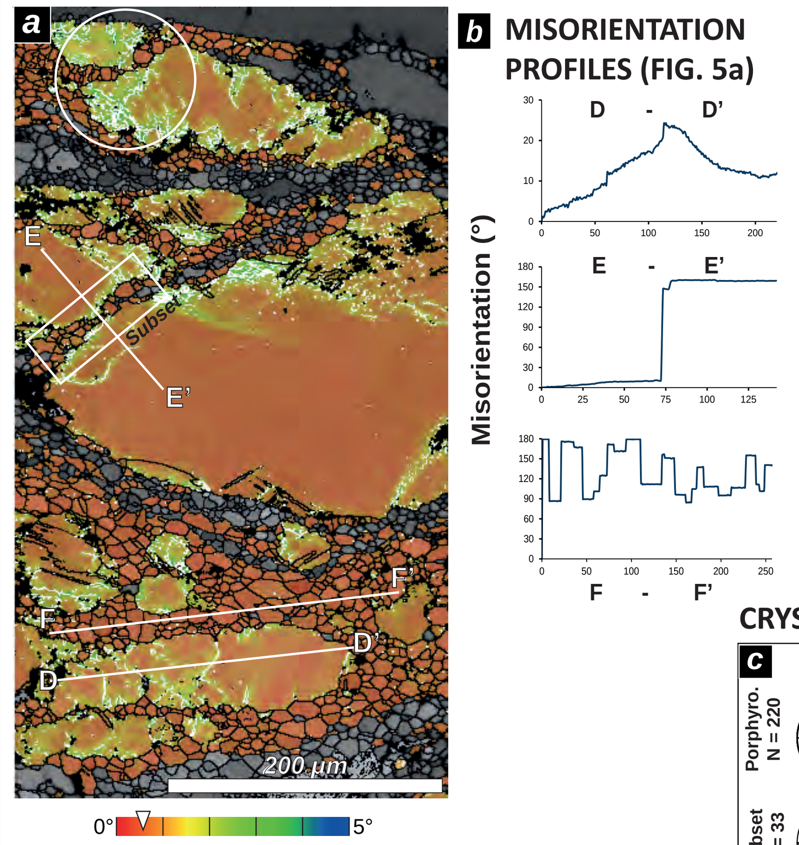


LOCAL MISORIENTATION MAP

Fig.5a - Local misorientation map, showing the misorientation angle (0-5deg) between adjacent pixels. Internal substructures and strain.

Fig.5b - Misorientation profiles across grains. Profile D-D' shows the strong lattice distortion across porphyroclasts, whereas profile E-E' and F-F' show the jumps of orientations across the fine-grained aggregate.

Plagioclase porphyroclasts display a weak CPO of {011} planes parallel to foliation. Intracrystalline bands of fine-grained plagioclase is not controlled by the porphyroclasts (Fig. 5c).

**CRYSTALLOGRAPHIC ORIENTATION OF PLAGIOCLASE**

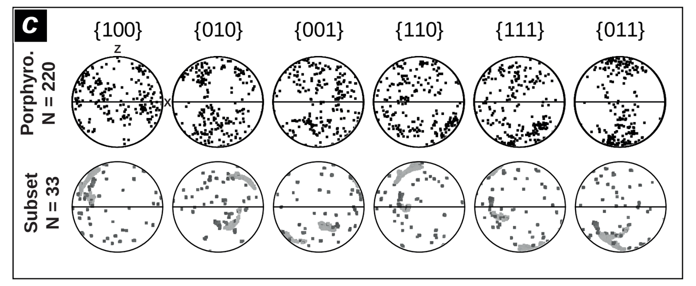


### 6. CLINOPYROXENE PORPHYROCLASTS

Clinopyroxene porphyroclasts do not show an obvious CPO (Fig. 6a). As for orthopyroxene, the fine grained aggregate rimming the porphyroclasts is highly misoriented, lacks a CPO and is not host controlled (Fig. 6a, b).

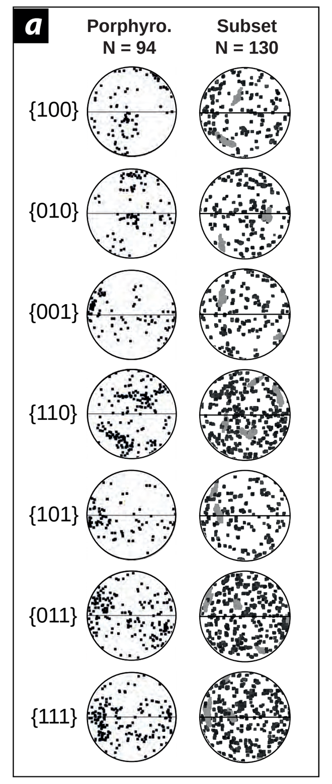


The misorientation profile confirms the jumps in misorientation between porphyroclasts and fine-grained aggregate (Fig 6b).

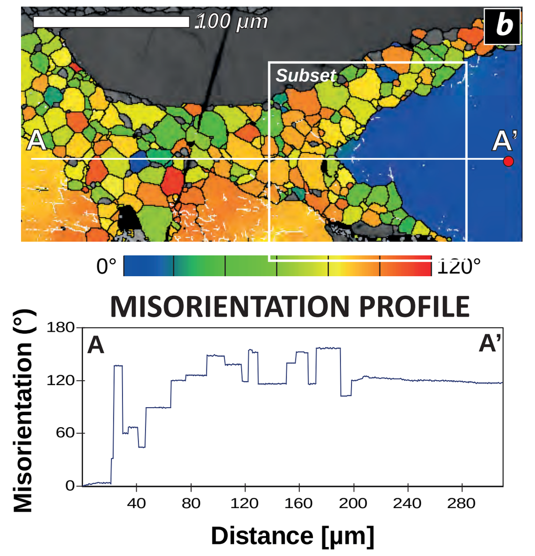


### 7. FINE-GRAINED POLY-PHASE MIXTURE

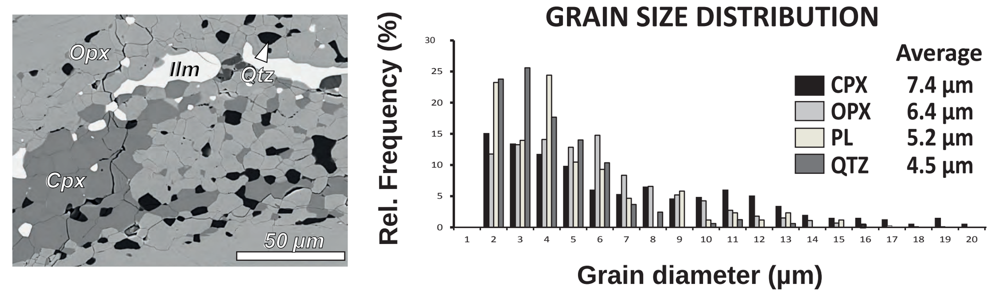


All phases of the polyphase mixture display a weak CPO (Fig. 7a)
**Opx:** maxima of {100} planes parallel to foliation and [001] directions parallel to stretching lineation, suggesting the {100}[001] slip system.
**Pl:** maxima of {011}, {111} and {110} planes parallel to foliation.

The misorientation angle distribution for uncorrelated pairs approaches that of the theoretical random curve, whereas for correlated pairs a modest increase of small misorientations can be observed (Fig. 7b).

**CRYSTALLOGRAPHIC ORIENTATION OF FINE-GRAINED AGGREGATE**

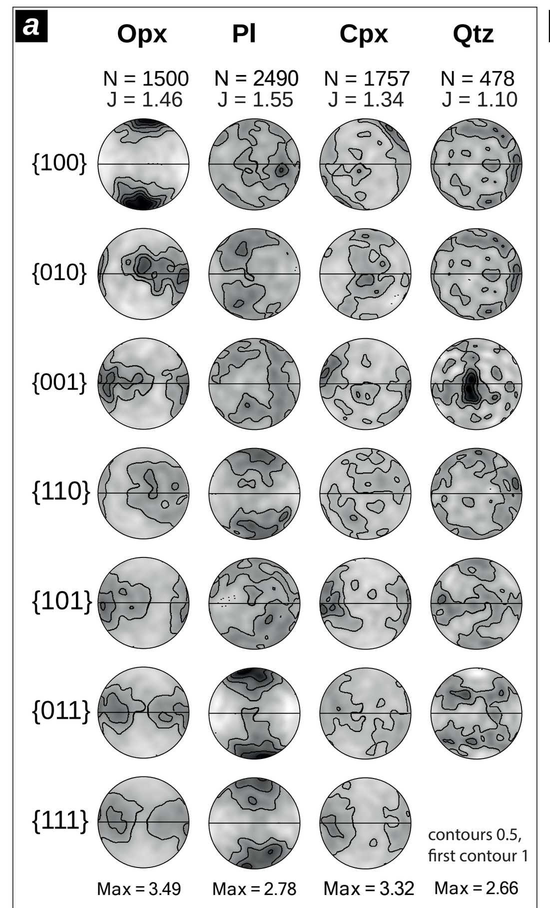


**MISORIENTATION ANGLES DISTRIBUTION**

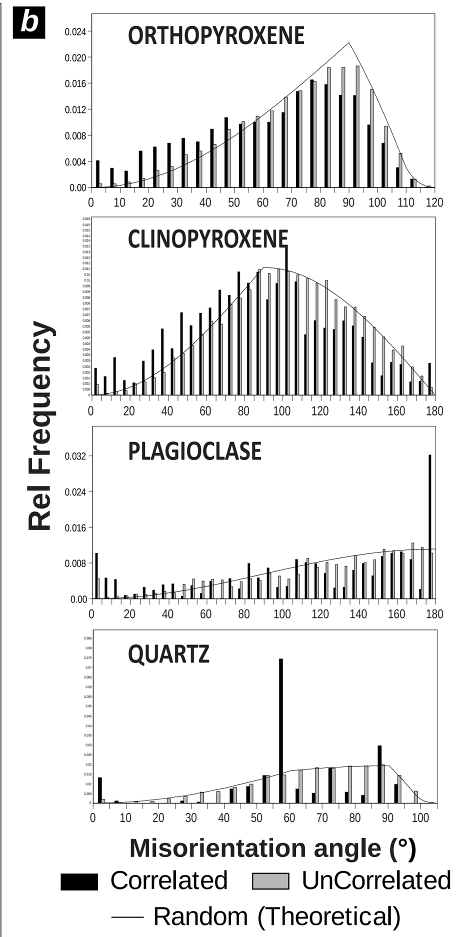


## 8. DYKE'S COMPOSITION AND MINERAL CHEMISTRY

**DYKE'S COMPOSITION COMPARED TO LEUCOSOME'S AND OTHER COEVAL DYKES**

The dyke's composition is intermediate between other dykes of the same generation (from Reginiussen et al. 1995) and the leucosomes of Menegon et al. (2011) indicating a degree of melt-rock interaction.

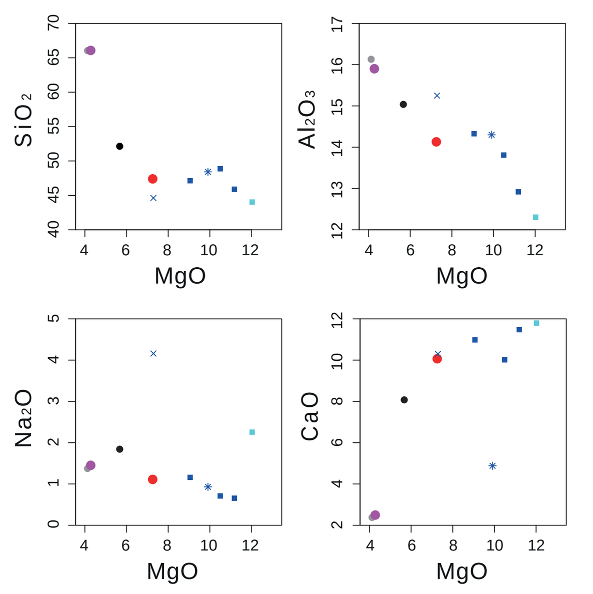


- O34b.2 without felsic • O23b.1 with felsic veinlet
- Menegon et al. 2011 Leucosome-rich domain
- Menegon et al. 2011 Leucosome-poor domain
- Reginiussen et al. 1995 Pre-kinematic dykes
- Reginiussen et al. 1995 Syn-kinematic dykes

**MINERAL CHEMISTRY OF PYROXENES AND FELDSPARS**

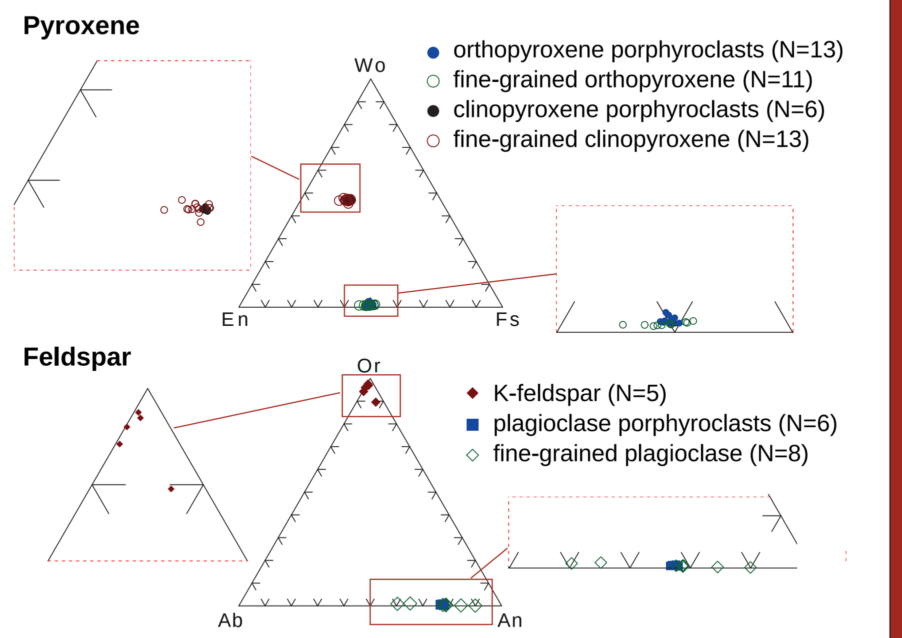


Porphyroclasts are homegeneous in composition.
Clinopyroxene: Diopside
Orthopyroxene: Ferro-enstatite (En50)
Plagioclase: Bitownite (An77)

Pyroxene in the fine-grained aggregate displays minor chemical variations from the porphyroclasts, whereas plagioclase shows relevant chemical variations ranging from An60 to An90.

## 9. MELT-ROCK INTERACTION FORMING FINE-GRAINED AGGREGATE

**MODELLING MELT-ROCK INTERACTION WITH THERMODYNAMIC MODELLING**
**modelling the chemical mixture between the mafic dyke and leucosome** (using Perple X, Connolly 1990)

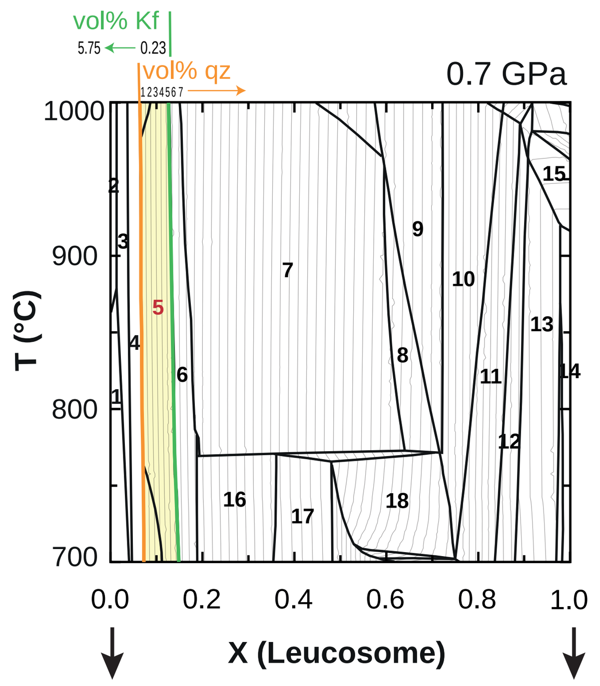


COMPOSITION A:
Reginiussen et al. 1995
pristine dyke 574C

COMPOSITION B:
Menegon et al. 2011
leucosome

**HOW DID THE FINE-GRAINED POLY-PHASE MIXTURE FORM?**

At the modelled conditions (0.7GPa and 700<T<1000), the fine grained poly-phase mixture observed in our dyke can be the result of melt-assisted metamorphic reactions for melt contents between 7-15 wt% (Field 5- in yellow).

The presence of K-feldspar and quartz delimit the stability field: K-feldspar is not stable on the right of the green line and quartz is not stable on the left of the orange line.

1. Opx, Bio, Pl, Grt, Cpx, Kf, Ilm
2. Opx, Bio, Pl, Ol, Cpx, Kf, Ilm
3. Opx, Bio, Pl, Cpx, Kf, Ilm
4. Opx, Bio, Pl, Cpx, Kf, Ru, Ilm
5. Opx, Bio, Pl, Cpx, Kf, Qtz, Ru, Ilm
6. Opx, Bio, Pl, Cpx, Qtz, Ru, Ilm
7. Opx, Bio, Pl, Cpx, Qtz, Ru, Ilm, H2O
8. Opx, Bio, Pl, Cpx, Qtz, Ilm, H2O
9. Opx, Bio, Pl, Cpx, Qtz, H2O
10. Opx, Bio, Pl, Qtz, H2O
11. Opx, Bio, Pl, Grt, Qtz, H2O
12. Bio, Pl, Grt, Qtz, H2O
13. Bio, Pl, Grt, Sill, Qtz, H2O
14. Bio, Pl, Sill, San, Qtz, H2O
15. Bio, Pl, Grt, Sill, San, Qtz, H2O
16. Opx, Bio, Amph, Pl, Cpx, Qtz, Ru, Ilm, H2O
17. Opx, Bio, Amph, Pl, Cpx, Qtz, Ilm
18. Opx, Bio, Amph, Pl, Qtz, Ilm, H2O

## REFERENCES

Elvevold et al. 1994, Journal of Metamorphic Geology, Vol.12
Menegon et al. 2011, Journal of Geophysical Reseach, Vol. 116, B10410
Reginiussen et al. 1995, Geological Magazine, Vol. 132, pp. 667-681
GCDkit: Janousek et al. 2006, Journal of Petrology, Vol. 47 (6), pp. 1255-1259
Perple X: Connolly 1990, American Journal of Science, Vol. 290, pp. 666-718